2023 IEEE International Conference on Robotics and Automation (ICRA 2023)
May 29 - June 2, 2023. London, UK

An underwater jet-propulsion soft robot with high flexibility driven by water hydraulics

Siqing Chen, He Xu*, Xiao Xiong, Ben Lu

Abstract— **Compared with rigid robots, soft robots have the advantages of inherent compliance, high adaptability, and impact tolerance. Many researchers are very interested in the motion design of soft robot underwater. In this paper, inspired by the method of octopus propulsion, a jet propulsion unit with 80% soft materials driven by pressure is designed. It can change the volume of its cavity to absorb and eject the fluid medium to make the robot move. According to the working characteristics of the jet unit, corresponding experiments are designed to analyze its force output, deformation, ejection flow, and pressure response characteristics. In order to expand the motion space of the robot, a buoyancy unit is designed to control the depth of the robot in the water. Three jet units and a buoyancy element are combined into a tetrahedron robot - jet soft robot (JSR). The feasibility of its motion is verified by experiments. Compared with other similar jet robots, the biggest feature of this robot is that the drive unit can bend or twist roughly along the centerline, which can prevent accidental collision and damage.**

I. INTRODUCTION

Due to its own inherent compliance, high adaptability, and impact tolerance, soft robots have unique advantages in ocean exploration.[1] Compared with rigid robots, soft robots are safer and more friendly to the environment and human operators.[2] The development and utilization of the ocean attracts many researchers to research the underwater soft robot.[3][4] The underwater movement of soft robot is an important research for the development of soft robot.

The movement of underwater soft robots includes driven by a propeller [5][6]; the fin-like mechanism reciprocating swing [7][8]; the high-pressure medium jet [9]; buoyancy [10][11]; crawling by a multi-leg mechanism [12][3]. Fan et al. [13] designed a articulated pneumatic actuator to realize the miniaturization of the bionic frog robot, through the study of frog biological structure and collective motion characteristics. Huang et al. [14] proposes a reconfigurable ontologically aware soft origami module that implements two basic driving modes (stretching and bending). They used five origami modules to assemble the smart jellyfish, complete with buoyancy adjustment and underwater grasping functions. Wood et al. [15] builds a sea urchin bionic robot to develop and demonstrate movement, inspired by sea urchin control pins and spines. The equatorial ring of the spine enables the robot to achieve yaw motion. Different method of motion have advantages and disadvantages.

Siqing Chen, He Xu, and Xiao Xiong are with the College of Mechanical and Electrical Engineering, Harbin Engineering University, China. Ben Lu is with with the Laboratory of Cognition and Decision Intelligence for Complex Systems, Institute of Automation, Chinese Academy of Sciences, China. Corresponding to He Xu: railway_dragon@sohu.com

In the ocean, soft creatures, like squid, octopus, and squid, have great athletic abilities and environmental adaptations. Inspired by this type of marine organisms, a type of actuation method that changes its own cavity to inject high pressure fluid has been proposed by many researchers. Federico et al. [16] designed a bionic jet propulsion driver that uses a motor to drive fibers to contract the bladder. Wang et al. [17] designed a prototype scallop robot that can clap and swim, inspired by the scallop's powerful underwater propulsion mechanism. Caleb et al. [18] proposed an AUV with a soft body to achieve repeatable jet propulsion by changing its internal volume and cross-sectional area, using jet propulsion and added mass effects. Yang et al. [19] proposed an origami inspired robot. It can change its body shape to absorb and expel water, creating a jet that pushes it forward, similar to a cephalopod. They used a magic ball origami pattern, which can switch between ellipsoidal (small volume) and spherical (large volume) shapes. In these designs, the special structure is used to store the fluid medium and pressurize it for propelling, which provides inspiration for our work. However, because the driving part relies on rigid parts, these kind of jet actuators is easy to be damaged due to impact or bending. This does not conform to the compliance characteristics of mollusks.

In this paper, we propose to use soft hydraulic machinery to replace the above rigid machinery. The jet unit can bend and twist very roughly without affecting the propulsion effect. Its 80% of the parts are soft materials. Our pressure supply system can be move to any place by tubes, which means that soft units can protect the rigid pressure system. A tetrahedral jet soft robot (JSR) is designed as the application of this unit. It consists of three jet units and one buoyancy unit, which can swim underwater. This paper focuses on verifying the feasibility of the design, and the arrangement of pressure supply is a future study. Therefore, control umbilical is selected to transmission pressure.

II. ACTUATE THEORY

According to the motion theory of jet robot, the forward motion is propelled by means of jetting fluid medium. The working theory of the jet unit is shown in Fig. 1. Jet unit has the ability to contract and recover. In the released state, the central actuator in pressurized is stretched and radial inflating, causing the volume of the work bladder reduced. The fluid medium is ejected, propelling the structure forward. In the energized state, the center actuator remains low pressure. The elongated actuator naturally rebounds by its material properties, making the volume of work bladder

restored. The fluid medium flows into the cavity, readied for the next jet cycle.

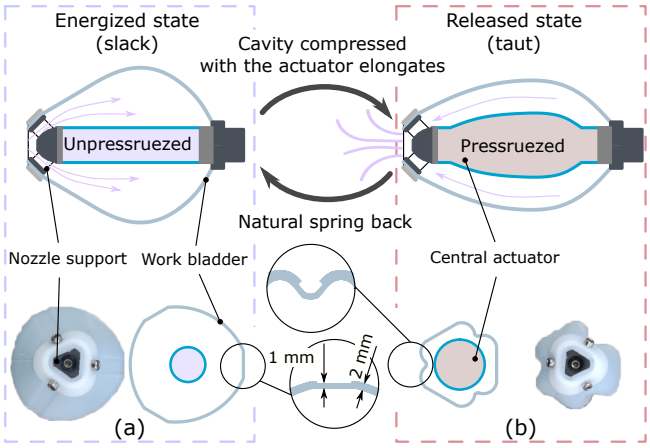

Fig. 1. Working theory of jet unit. a) With actuate bladder's pressure losing, the expanded elastomer pulls back to the nozzle support. The volume of work bladder becomes larger. The hydraulic medium is sucked into the unit. b) Actuate bladder is pressurized and expanded to make the movement of nozzle support. The volume of work bladder is reduced. The hydraulic medium is ejected. These two working states form a cycle to generate the push force.

To reduce the interference to work bladder in the released state, a trench structure is designed. The work bladder is a sphere-like body formed by alternating combination of three pieces of silicone (connecting part) with a thickness of 1 mm and three pieces of silicone (main part) with a thickness of 2 mm. With the stretching and rebounding of center actuator, the structure of work bladder can transform between two forms: ellipsoid-like and sphere-like. As shown in Fig. 1(b), with work bladder elongated, because the stiffness of the connecting part is lower than that of the main part, its deformation depends on main part. The main part loses the spherical curvature and bends to the connecting parts on both sides. The connecting part guides the bending of main body to the trench, to adapt the deformation of work bladder. In this state, the JU transforms into an ellipsoid-like shape.

The deformation state of work bladder is controlled by three parameters: its surface function in the relaxed state, the proportion of the body part, and its thickness. They all affect the volume of work bladder, relaxation stability, taut compliance. In this study, we selected the parameters through experiments and experience. The deformation optimization of work bladder is our future research.

III. Fabrication

A. Jet unit

Fig. 2 shows the fabrication process of jet unit. Its soft part consists of actuate bladder for the center actuator and work bladder for flow in and out of fluids. The soft part is cured by silicone. The silicone (Smooth-ON SIL 936, by smooth-On Inc.) with a shore abrasion of 36 A is chosen as the soft material. The mold is made by 3D printing. The vacuum pump is used to remove the bubbles in the fluid silicone during the whole process. Fig. 2(a-b). shows the fabrication process about tubular main body and sealed connection of actuate bladder. To connect the nozzle with it, the connection method between the rigid part and the silicone proposed by Rossing et al.[20] is applied. The pressure input method is used to connect pressure input parts and actuate bladder. The actuate bladder is assembled according to Fig. 2(c) to form the central actuator.

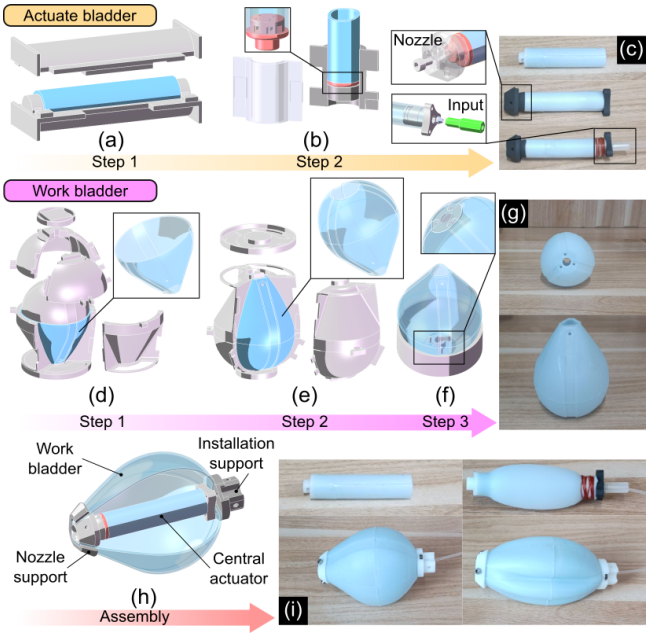

Fig. 2. Fabrication steps of the jet unit. Actuate bladder: a) molding process of the main body, b) sealed connection process, and the c) real products; Work bladder: d-e) molding process of the main body, f) bottom sealing process, and its g) Real products; h) assemble model of JU; i) working condition of JU.

The work bladder is a channel with a very small opening. All-in-One forming technology cannot remove the mold core. In this research, the main body of work bladder is made in two steps, leaving a larger opening at the bottom for taking out the mold core. The sealing base is formed in the bottom mold, combined as one part relying on the curing characteristics of the silicone. The bottom mold is reserved with mounting holes. The production process of work bladder is presented in Fig. 2(d-f). The final work bladder is shown in Fig. 2(g).

The central actuator and the work bladder are assembled as jet unit, shown in Fig. 2(h). The jet unit contains a work bladder for storing the pushing fluid medium, a nozzle support for guiding the fluid, a Installation support for connecting with other components, and a central actuator that provides the main shrinkage and resilience force. Fig. 2(i) shows the working state of jet unit. Due to the sealability caused by the compressibility of the silicone, the fluid medium can only enter and exit through the nozzle. The thrust provided by jet unit depends on the flux q of the fluid medium, which can be expressed as:

$$F_t = C\rho A q^2 \tag{1}$$

Where ρ is the density of the fluid medium; A is the area of the nozzle outlet; $C < 1$ is the propulsion efficiency, which is related to the friction at the nozzle and flow loss in work bladder. The jet unit has a certain power. The work bladder volume changes are used for jet behavior during deformation. The flux is inversely proportional to the area A. We build up a simple mathematical model to optimize and calculate the relevant parameters for the maximum output force.

B. Buoyancy unit

The manufacture of the buoyancy unit is divided into the main body and the connecting part. The main body of the cavity is a trapezoidal structure. The mold core is a concave polyhedron. The process is achieved by means of splicing molds. The shell molds are divided into four parts, and make the bladder main body through the internal core and the external mold core, as shown in Fig. 2(a). The silicone body is placed on the bottom mold as shown in Fig. 2(b). The bottom of the main body is sealed, leaving a sealed pipe to connect the pressure inlet. The structure of the pressure inlet of the buoyancy unit is the same as that of the central actuator, including preload contact, DS contact, and cone contact.[4] DS contact is applied to support the bladder. Preload contact is used to squeezing the cone contact. Cone contact is made of soft material, which seals the gap between the pipe and the DS contact after being preloaded. The final buoyancy unit is shown in Fig. 2(c). Its maximal volume change reaches 2.18 times.

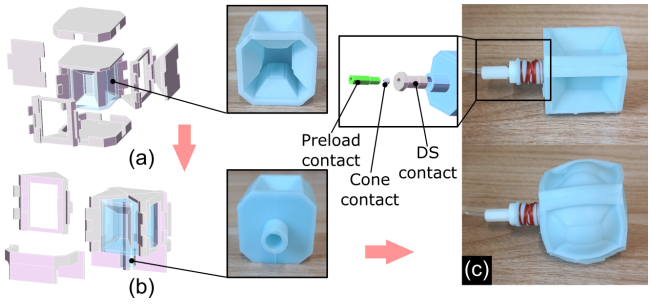

Fig. 3. The fabrication process of BU (buoyancy unit): a) main body and b) connecting part; and its c) working state.

C. jet soft robot

According to Fig. 4(a), buoyancy unit and jet unit are assembled as the jet soft robot (JSR). The installation support of jet units are connected with the central support. The pressure inlet of the buoyancy unit is clamped by the center support. JSR consists of three jet units and one buoyancy unit. The centerline of each units are arranged in the centerline of a regular tetrahedron. Jet unit's soft material providing the JSR with drop resistance. The arrangement of jet unit's tripod makes the JSR adaptable to various underwater environments. The buoyancy unit sits above the JSR and provide buoyancy by inflating own cavity. All chambers are supplied with pressure medium through the control umbilical. To maintain the stability of JSR in water, the working medium of jet unit is water, and the buoyancy unit's is air.

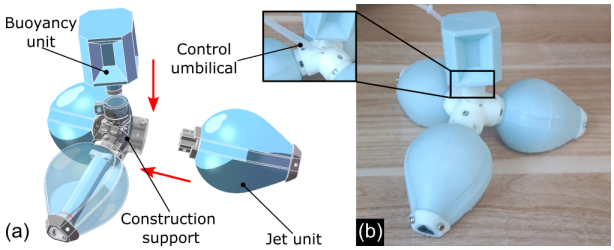

Fig. 4. a) JSR (jet soft robot) assembly process; and the b) real products.

IV. Experiment And Analysis

A. Experimental setups

In this paper, we use a water hydraulic experiment platform to provide high pressure gas and water, shown in Fig. 4. The fluid is pressurized by the pump, and input to valve group to regulate and distribute the pressure.[21] A pressure of 100 KPa is chosen as the maximum working pressure. The pressure detected in the experiment is provided by a pressure transmitter (MEACON, Type MIK-P300). The blue section is used to measure the force output and flow output of the central driver and unit. The HANDPI (HLD0824) dynamometer is used to detect the fluid mass and the force generated by the actuator. The yellow part is applied to measure the thrust of jet unit, which is measured by HANDPI (HLD2000) dynamometer. The red part shows the underwater environment simulated by tank, which is used for the motion experiment of JSR. The Dynamometers' sampling frequency is 10Hz, and their accuracy is 0.001N. The sampling frequency of the pressure transmitter is 10hz, and its accuracy is 0.1 KPa. Two cameras (SAMSUNG HMX) outside the tank is applied to capture the position of JSR in two mutually perpendicular directions, so as to estimate the spatial position of the JSR.

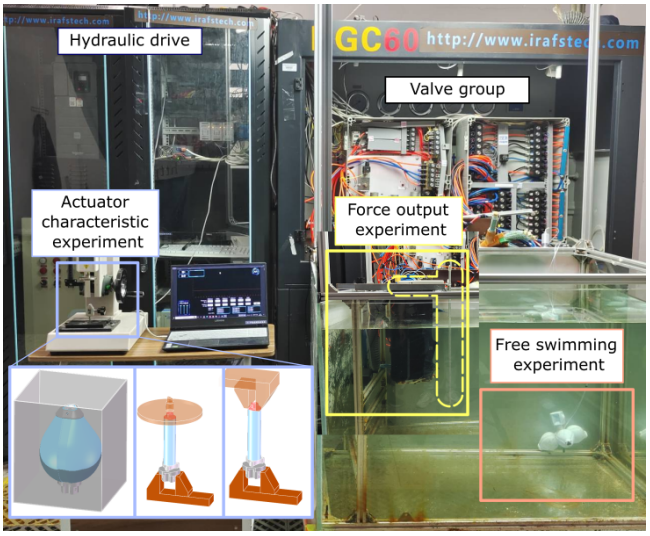

Fig. 5. The experimental platform and the test environment.

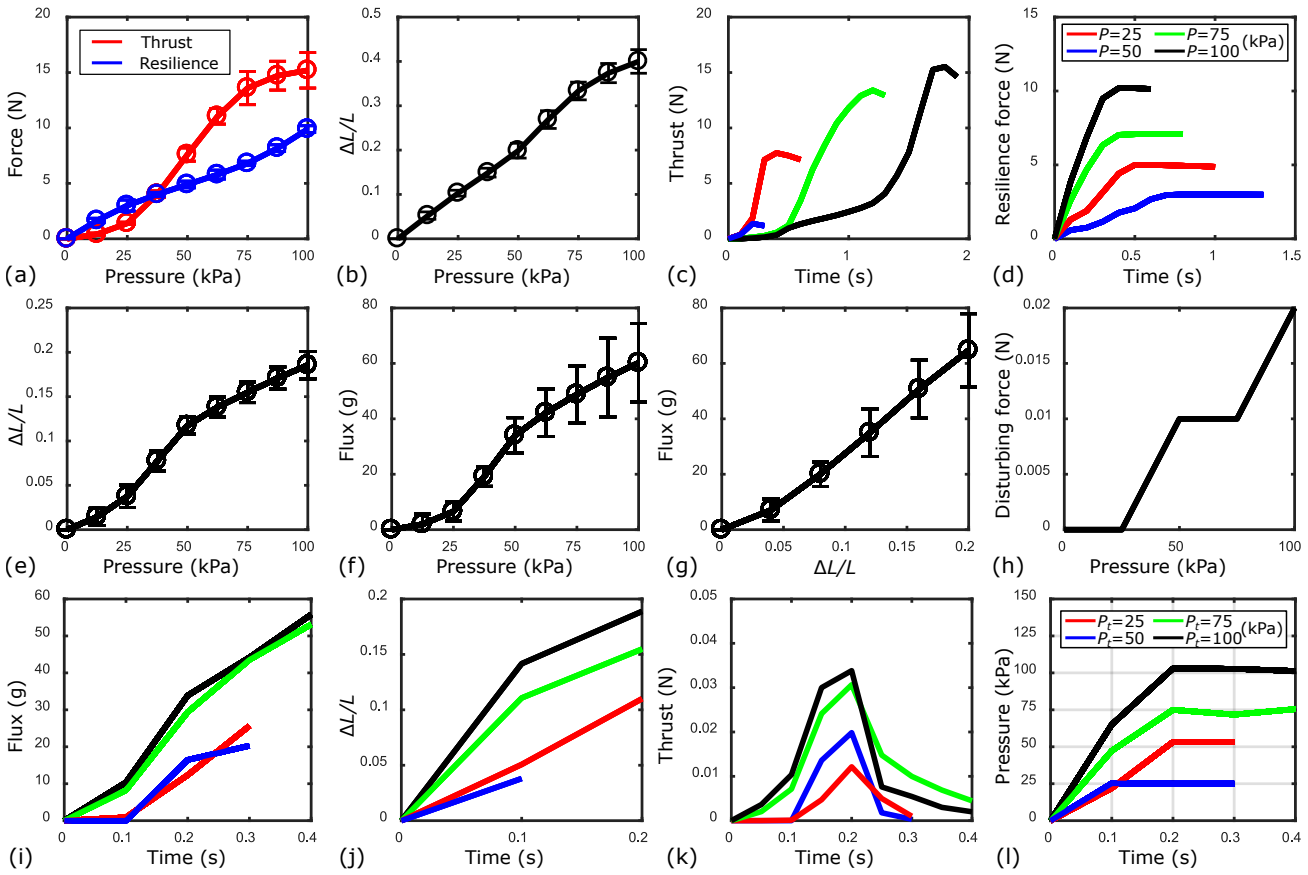

Fig. 6. Characteristic of the central actuator: a) force output state and b) elongation after pressure stabilization; its transient c) thrust and d) resilience force output with different target pressures, where the legends of Figure (c-d) are the same. Characteristic of jet unit: e) elongation and f) mass of the hydraulic medium pushed out after pressure stabilization; g) relationship between the elongation state and the mass of the hydraulic medium ejected; h) maximum disturbance force after difference pressure release; its transient i) ejected hydraulic mass, j) elongation, k) output thrust, and l) pressure input with different target pressures, where the legends of Figure (i-l) are the same.

B. Test for jet unit

The experimental results are shown in Fig. 6 The properties of jet unit depend on the deformation of the central actuator. The elongation properties, force-output properties, and transient mechanical properties of central actuator are analyzed by comparing the effect of support on the efficiency in jet unit. All steady experiments are validated 10 times.

In the thrust experiment, one end of the central actuator is fixed and the other end is free to extend. The dynamometer is moved to the free end position. Central actuator is fed the pressure medium slowly. With the pressure stabilizing at the target pressure, the dynamometer starts to measure. In the tensile test, one end of the central actuator is fixed and the other end is free to stretch. The fluid medium with the target pressure is input into the central actuator, keeping the deformation stable. The dynamometer is moved to the free end position. The pressure in central actuator is release to standard atmospheric pressure. In the states of the central actuator stable, the dynamometer starts to measure. The experimental results of steady force output with different pressure are shown in Fig. 6(a). The thrust is caused by the central actuator's axial expansion. Silicone has the greatest elastic potential energy when it starts to stretch. Its resistance to pressure causes the thrust to grow slowly. With the pressure of 70 KPa, the silicone enters the yield limit. Its deformation increase in a small range. With the pressure of $30 \sim 70$ KPa in central actuator cavity, the thrust have a degree of the linearity.

In the elongation experiment, the methods of the central actuator fixation and pressure supply are the same as in the thrust experiment. In the initial state of central actuator, and its pressure and the deformation stable, the displacement of the free end in the central actuator is measured, respectively. The characteristic between elongation and pressure is shown in Fig. 6(b). The elongation deformation of the central actuator is only related to the end area and pressure, so the elongation characteristic curve shows an almost linear change. In this state, the resilience force is only related to the elongation length of the central actuator. Thus, the resilience characteristic is consistent with the elongation characteristic.

The transient mechanical characteristics experiments are shown in Fig. 6(c-d). Using the pressure control system in Fig. 5 to stabilize the pressure at the target value as soon as possible, the thrust changes are record. Due to the power limitation of the pressure system, the pressure loss of the central actuator pressure inlet, and the deformation response

of the silicone material, the thrust output with larger target pressure takes longer times to stabilize. The response speed of the resilience force in the depressurize state is related to the pressure difference. With greater the target pressure, the shorter the time for the resilience force to stabilize is taken. The drop in thrust at the peak may be caused by inertial effects. This is also the case in resilience force, with a smaller value. The end for each curve indicates that the subsequent thrust does not change anymore.

Jet unit's experiments focus on its eject flow characteristics, elongation characteristics, and thrust characteristics for jetting. All steady experiments are validated 10 times. In the steady elongation experiment, the installation support of jet unit is fixed. Its nozzle displacement is measured. Jet unit is supplied with pressure in the same method as in the previous steady experiments. Incomplete elongation of jet unit is caused by the obstruction of work bladder to central actuator with high pressure. Therefore, with the pressure of the fluid medium more than 50 KPa, the elongation of jet unit becomes slower. The relationship between pressure and elongation is presented in Fig. 6(e).

In the steady flow experiment, the work bladder of jet unit is filled with fluid medium and placed vertically in a glass container, shown in Fig. 5 (blue box). The flow is estimated by measuring the mass of the fluid ejected. This method of flow measured is not precise. But its mechanical properties can be estimated. The relationship between pressure and flow is presented in Fig. 6(f). The relationship between the elongation of jet unit and the ejected flow is shown in Fig. 6(g). The growth trends of flow (Fig. 6(e)) and elongation (Fig. 6(f)) are similar under pressure changes, so the trend of Fig. 6(g) is close to a linear change.

According to the above experimental configuration, the pressure shown in Fig. 6(l) is input into central actuator of jet unit, where P_t represents the target pressure. Ideally, the pressure should reach the target pressure at $t = 0$. The main reasons for the pressure delay and fluctuation are caused by the power limitation of the pressure system, the pressure loss of the connecting pipeline, and the response delay of the elastomer. The end of each curve represents no subsequent pressure change.

Fig. 6(i) shows the ejected fluid mass with time for different target pressures. Jet unit's maximum response time is 0.4s. It is sufficient to select 0.5s as the pressurization time during the subsequent JSR swimming. The higher pressure fluid medium makes jet unit respond more quickly to play the jet motion. The low pressure fluid needs to resist the pressure loss along the way, and the large elastic potential energy. So low pressure response is always slower than high pressure's. We reiterate that the timeliness and accuracy of flow experiments are very poor, but the mechanical properties can be analyzed through its trends.

Fig. 6(g) shows that flow can be inferred from elongation in steady state. Thus, Fig. 6(j) can represent the trend of the transient flow. The end of each curve indicates that the length of the subsequent jet unit does not change anymore. However, after the length of jet unit stable, the fluid medium is still ejected due to the elastic effect of work bladder. Therefore, the above results are discussed in conjunction with Fig. 6(i) and Fig. 6(j).

In jet unit's propulsion characteristics, the thrust is captured by the structure shown in Fig. 5 (yellow box). This is the method used by many researchers [16][18]. The transient thrust is shown in Fig. 6 (k). With the ejection of the flow, the thrust in different target pressures reaches the maximum at about 0.2s. Jet unit's thrust is calculated by Eq. 1. At high pressure, there is little difference in the flow of the Jet unit ejection. Therefore, the output thrust difference at higher target pressure is also small. For the economy and safety, the driving pressure of jet unit is not as big as possible. In this study, the disturbing force of jet unit during water absorption is attempted to be measured, which is shown in Fig. 6(h). Due to the precision of the measuring instruments, the transient forces are hardly statistically significant. To exclude the interference of the disturbing force, the rated working pressure of jet unit is selected as 100 KPa.

Fig. 7 shows the velocity contour of the maximum jet state in one cycle simulated by CFD. ($P_t = 100$ KPa) The simulation is verified by mesh independence. Compared with the real jet water wave, the hydrological shape is very close ($v = 0.1$ m/s). The simulated thrust force is 0.048 N, and the mass of eject flow is 76.3 g. The actual measured maximum thrust is 0.034 N, and the eject flow is 58.6 g.

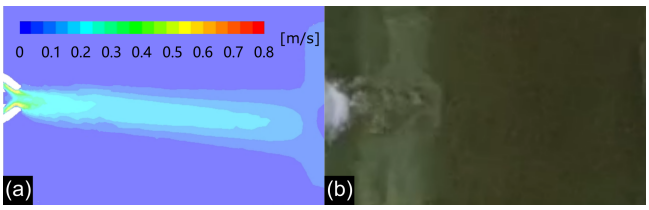

Fig. 7. a) CFD simulation for water jet; b) the water wave of the actual jet.

C. Motion experiment for jet soft robot

In the motion experiment, JSR is controlled to float on the water, and its jet unit completely sinks in the water. First, JSR is input with a pressure of 100 KPa within 0.2 s, so that its jet unit is elongated by 18%. Secondly, after maintaining the high pressure of central actuator for 0.5 s, the hydraulic medium in the work bladder is ejected. Then, the pressure in central actuator is slowly released to standard atmospheric pressure within 0.5 s. Finally, after 0.8 s, the work bladder returned to its maximum volume and filled with fluid medium, readying for the next cycle. Each control cycle of JSR lasts 2 s. The JSR moves in the water with an average speed of 24 mm/s in the X direction, which translates to 0.23 body lengths/s. Fig. 8(a-b) shows the trajectory of the center of JSR. During 6 control cycles, JSR move to X direction with the distance of 192.9 mm in jet unit actuating, and offsetting the distance of $-2.9 \sim 29.4$ mm in the y-direction.

We must declare that control umbilical play a very large interference on the movement of the JSR. It limits the space

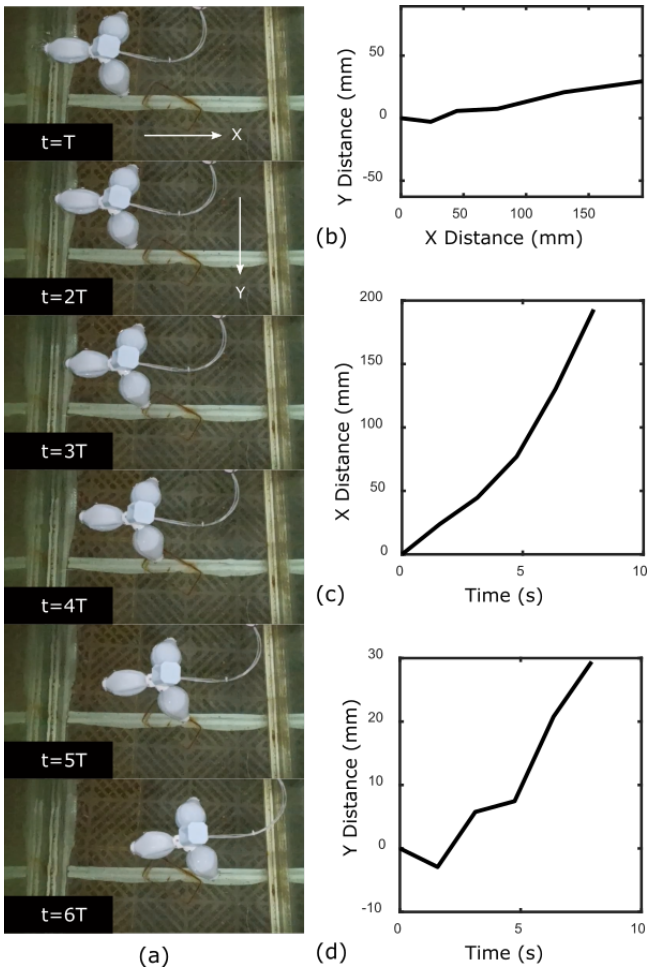

Fig. 8. a) snapshots of the robots motion, where $T = 2 \pm 0.5$ s; b) trajectory of the JSR center on Plant XOY; the robots c) x and d) y position over time.

of JSR's movements, and has a very serious obstacle to the movement of JSR. In this experiment, the control umbilical produced a maximum interference force of 0.031 N, towards its radial direction. This force is the same order of magnitude as jet unit's maximum thrust. In special cases, the JSR with control umbilical swings in the same position. From the second control cycle, the movement of the JSR begins to be restricted by the control umbilical. Finally, under the action of the ju thrust and the umbilical cord, the JSR begins to shift in the positive direction of Y. The cableless design of JSR is the focus of future research.

D. Potential application

Fig. 7 shows the application of buoyancy unit and jet unit. As shown in Fig. 7(a), through the inflating of the buoyancy unit, the JSR can control its depth in the water, which provides the robot with 3-dimensional freedom of movement. As shown in Fig. 7(c), after JSR floated through the buoyancy unit, it moved 286 mm horizontally with the push of the jet unit, and slowly landing on the bottom of the water. Its maximum floating speed and sinking speed reach 98 mm/s and 52 mm/s, respectively. Its movement trajectory is 'n' type. Applied with the buoyancy, JRS can sink into the water for tasks such as underwater exploration, and the thrust generated by their units give it three-dimensional maneuverability. Due to the soft material of JSR, the drive part can resist a violent hit and recover quickly, as shown in Fig. 7(b), which can prevent accidental collision and damage. Even 90° of large deformation and bending, JSR still work normally. This is the advantage of JSR over other water-jet type robots.

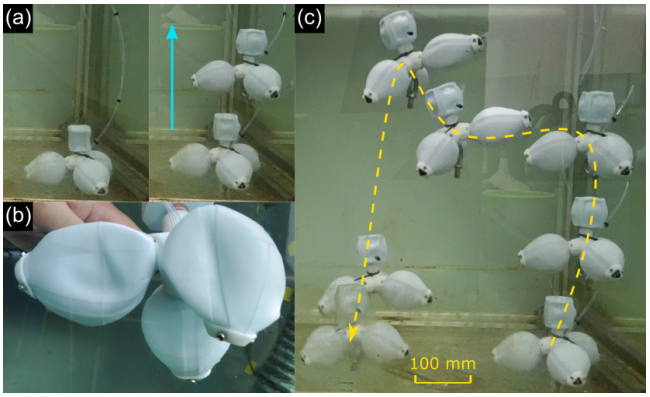

Fig. 9. a) floatation experiment; b) highly flexible of JST, which can be bent at will; c) applications of floating and jet propulsion.

V. Conclusion

In this paper, we present a pressure-driven jet-propelled drive unit (jet unit). It is combined with the buoyancy system (buoyancy unit) to form a tetrahedral soft robot (JSR) capable of swimming freely in the water, with a horizontal movement speed of 24 mm/s, a maximum floating speed of 98 mm/s, and a sinking speed of 52 mm/s. JSR's jet units suck in hydraulic medium from the outside, relying on its own pressure structure to eject the fluid out of the cavity, which propel the JSF forward. Jet unit's cavity can store 160 g of water. In working conditions, it can eject the fluid up to 37% out the cavity, generating a maximum thrust of 0.034 N. This thrust can be made larger by optimizing the pressure system in future. Comparing with other similar jet robots, 80% of the parts of the unit of JSR are soft structures. JSR's drive units (both jet and buoyancy unit) can tolerate very violent bending, twisting, and bumping. This may provide inspires for soft robots to move underwater.

In future work, we will focus on the cableless realization of soft robots. The miniaturization and underwater arrangement of the pressure system are research in depth. Further optimization of the design parameters of the cavity extrusion type of jet propulsion is carried out to improve the efficiency of underwater movement of the robot.

Acknowledgment

This work was supported by the Natural Science Foundation of China under Grant 51875113, Natural Science Joint Guidance Foundation of the Heilongjiang Province of China under Grant LH2019E027. This paper is funded by the International Exchange Program of Harbin Engineering University for Innovation-oriented Talents Cultivation.

REFERENCES

[1] S. Aracri, F. Giorgio-Serchi, G. Suaria, M. E. Sayed, and A. A. Stokes, "Soft robots for ocean exploration and offshore operations: A perspective," *Soft Robotics*, 2021.

[2] L. Ren, B. Li, G. Wei, K. Wang, and Q. Liu, "Biology and bioinspiration of soft robotics: Actuation, sensing, and system integration," *iScience*, vol. 24, no. 9, p. 103075, 2021.

[3] S. Mao, E. Dong, S. Zhang, X. Min, and Y. Jie, "A new soft bionic starfish robot with multi-gaits," in *IEEE*, 2013.

[4] H. Wang, H. Xu, F. Yu, X. Li, C. Yang, S. Chen, J. Chen, Y. Zhang, and X. Zhou, "Modeling and experiments on the swallowing and disgorging characteristics of an underwater continuum manipulator," in *2020 IEEE International Conference on Robotics and Automation (ICRA)*, 2020, pp. 2946–2952.

[5] C. Zavislak, A. Keow, Z. Chen, and F. Ghorbel, "Auv buoyancy control with hard and soft actuators," in *2021 American Control Conference (ACC)*, 2021.

[6] T. S. Kim, J. Kim, and S. C. Yu, "Design of a buoyancy controllable auv by changing volume for data collection in the water column," in *IEEE/OES Autonomous Underwater Vehicle Workshop*, 2018.

[7] G. Li, X. Chen, F. Zhou, Y. Liang, Y. Xiao, X. Cao, Z. Zhang, M. Zhang, B. Wu, and S. Yin, "Self-powered soft robot in the mariana trench," *Nature*.

[8] Y. Wang, L. Loh, U. Gupta, C. C. Foo, and J. Zhu, "Bio-inspired soft swim bladders of large volume change using dual dielectric elastomer membranes," *Journal of Applied Mechanics*, vol. 87, no. 4, pp. 1–27, 2020.

[9] F. Renda, F. Giorgio-Serchi, F. Boyer, and C. Laschi, "Modelling cephalopod-inspired pulsed-jet locomotion for underwater soft robots," *Bioinspiration & Biomimetics*, 2015.

[10] Z. Ren, W. Hu, S. Dong, and M. Sitti, "Multi-functional soft-bodied jellyfish-like swimming," *Nature Communications*, vol. 10, no. 1, 2019.

[11] A. Joshi, A. Kulkarni, and Y. Tadesse, "Fludojelly: Experimental study on jellyfish-like soft robot enabled by soft pneumatic composite (spc)," *Robotics*, vol. 8, no. 3, p. 56, 2019.

[12] A. Faudzi, M. Razif, G. Endo, H. Nabae, and K. Suzumori, "Soft-amphibious robot using thin and soft mckibben actuator," in *2017 IEEE International Conference on Advanced Intelligent Mechatronics (AIM)*, 2017.

[13] J. Fan, S. Wang, Q. Yu, and Y. Zhu, "Swimming performance of the frog-inspired soft robot," *Soft Robotics*, vol. 7, no. 5, 2020.

[14] J. Huang, J. Zhou, Z. Wang, J. Law, H. Cao, Y. Li, H. Wang, and Y. Liu, "Modular origami soft robot with the perception of interaction force and body configuration," *Advanced Intelligent Systems*, vol. n/a, no. n/a, p. 2200081. [Online]. Available: https://onlinelibrary.wiley.com/doi/abs/10.1002/aisy.202200081

[15] T. Paschal, M. A. Bell, J. Sperry, S. Sieniewicz, and J. C. Weaver, "Design, fabrication, and characterization of an untethered amphibious sea urchin-inspired robot," *IEEE Robotics and Automation Letters*, vol. 4, no. 4, pp. 3348–3354, 2019.

[16] F. Renda, F. Giorgio-Serchi, F. Boyer, C. Laschi, J. Dias, and L. Seneviratne, "A unified multi-soft-body dynamic model for underwater soft robots," *The International Journal of Robotics Research*, vol. 37, no. 6, p. 027836491876999, 2018.

[17] Y. Wang, S. Pang, H. Jin, M. Xu, and S. Zhang, "Development of a biomimetic scallop robot capable of jet propulsion," *Bioinspiration & Biomimetics*, vol. 15, no. 3, p. 036008, 2020.

[18] C. M. Christianson, Y. Cui, M. Ishida, X. Bi, and M. T. Tolley, "Cephalopod-inspired robot capable of cyclic jet propulsion through shape change," *Bioinspiration & Biomimetics*, vol. 16, no. 1, 2020.

[19] Z. Yang, D. Chen, D. J. Levine, and C. Sung, "Origami-inspired robot that swims via jet propulsion," *IEEE Robotics and Automation Letters*, vol. 6, no. 4, pp. 7145–7152, 2021.

[20] A. Lr, B. Rbns, C. Bc, C. STXDETX, and B. Eld, "Bonding between silicones and thermoplastics using 3d printed mechanical interlocking," *Materials & Design*, vol. 186.

[21] S. Chen, H. Xu, and X. Zhou, "Bionic water hydraulic system of soft robot control inspired by spider limbs," in *2021 IEEE International Conference on Robotics and Biomimetics (ROBIO)*, 2021, pp. 719–725.